U.S. DEPARTMENT OF COMMERCE
NATIONAL OCEANIC AND ATMOSPHERIC ADMINISTRATION
NATIONAL WEATHER SERVICE
NATIONAL METEOROLOGICAL CENTER

OFFICE NOTE 342

SIMPLE MOUNTAIN WAVE EFFECTS IN THE NESTED GRID MODEL

NORMAN A. PHILLIPS
JAMES E. TUCCILLO

JULY 1988

During the period 00GCT 22 February 1988 through 00GCT 6 March 1988, the Nested Grid Model (NGM) was run in a parallel mode, for both 00 and 12 GCT runs, in addition to the operational runs. The parallel mode used the same analyses as the operational mode, but its forecast model included a simple parameterization of mountain wave drag. (The expression "mountain wave drag" is used to denote the effect of gravity waves that are generated in the atmosphere by flow over uneven terrain.) In the model, gravity waves generated by the explicity represented height field $\overline{h}$ can be assumed to be forecast by the model. Parameterization is needed however to account for gravity waves generated in response to unevenness of the terrain on horizontal scales shorter than that of $\overline{h}$. Figure 1, for example, shows the standard deviation of the height field from a locally averaged height field, as computed from the 10' tabulation from the U. S. Navy.

$$\overline{h'^2} = \overline{(h - \overline{h})^2} \qquad (1)$$

The overbar represents an average over a square of 1^o X 1^o . (This size is slightly smaller than the 83 km grid interval on the finest of the three forecast grids in the NGM.)

This drag has been shown to be important for medium range forecasts of the averaged zonal wind $\overline{u}$ (Palmer, Shutts, and Swinbank, 1986), especially in the stratosphere. Less is known about its importance for shorter forecasts and for models that have a moderately fine horizontal grid resolution of $\overline{h}$.

The parameterization used in the parallel NGM forecasts was very simple. The drag (i.e., stress) at the bottom of the atmosphere was defined as being opposite in direction to V, where V is the forecast wind averaged over the bottom six layers of the model (a pressure-thickness of about 300 mbs). The magnitude of the surface stress was based on the formula suggested by Pierrehumbert (1987):

$$\tau_o = [\rho V^3 / N L] G(Fr) \qquad (2)$$

N is the buoyancy frequency. L is a length typical of the horizontal wave length of the iregularities. G is a non-dimensional function of the Froude number Fr:

$$Fr = N h' / V \qquad (3)$$

Pierrehumbert suggests the following form for G

$$G(Fr) = G_{max} \times \frac{Fr^2}{a^2 + Fr^2} \qquad (4)$$

with

$$G_{max} = 1, \quad a^2 = 1 \qquad (5)$$

For $N = 10^{-2}$ sec^{-1}, $h' = 100$ m (See Figure 1), and V = 10 m/sec, Fr_2 is about 0.1 , so that (2) may be rewritten as b

$$\tau_o \sim \frac{G_{max}}{a^2} \frac{\rho V N}{L} \overline{h'^2}$$

$$= C \frac{\rho V N}{L} \overline{h'^2} \quad . \qquad (6)$$

The length L was set at 100 km, and some preliminary calculation suggested a value of 2 for C in the parallel runs.

The variation of the stress with height was very simple in these experimental runs:

$$\tau = \tau_o (p / p_o) \quad . \qquad (7)$$

This results in a body force on the atmosphere that is independent of height. (According to geostrophic adjustment theory, the major effect of this on the temperature field will depend on horizontal variations in τ , since much of $\partial \tau / \partial p$ can be balanced by the Coriolis force created by a slight change in the vertically averaged wind field. More detailed variations of τ with height are believed to arise from finite amplitude effects at low elevations and in the stratosphere, and at elevations where the wind begins to have a component in the negative direction of V .)

Figure 2 shows the mean 500-mb chart for this period. The skill, as measured by the 500-mb height anomaly correlation coefficient averaged over North America, was essentially identical (Figure 3) in the operational and parallel runs . The fields of mean 500-mb error and standard deviation of the 500-mb error were also almost identical. (Figures 4 and 5).

2. Circumstantial evidence as to the need for a better representation of τ .

A retrospective examination of some of the details suggested that the formulas (6) and (7) above were too simple. This conclusion was arrived at by the following device. An artificial forecast 'A' was defined as a linear combination of the parallel (P) and operational (O) forecasts, both of which had been recorded on disk:

$$A = \alpha P + (1 - \alpha) O = O + \alpha (P - O) \qquad (8)$$

A value of 1 for the parameter α corresponds to the full parallel forecast, while $\alpha = 0$ corresponds to the operational forecast. Values of α greater than 1 "correspond" to an increase in the drag, much as if the constant C in (6) had been increased above the value 2.

This device was applied to a range of α at each of the 4 standard surfaces 850, 700, 500, and 250 mbs. Each artificial forecast A was verified against the corresponding NGM 0-hour field. The error measure adopted for each level was the squared standard deviation of the error about its mean value, averaged over all cases and over North America. The results are tabulated in Table 1.

Table 1. Squared errors (about the mean error) in meter^2 for artificial forecasts with the tuning parameter α. The minimum value as a function of α is indicated with an asterisk. The sample size is 27. β is the ratio of the asterisked value to the value for α=0, i.e. the operational forecast.

	250 mbs					500 mbs			
α	12hr	24hr	36hr	48hr	α	12hr	24hr	36hr	48hr
0.0	396.6*	1083.3	2126.3	3557.4	0.0	304.4	769.1	1489.0	2479.4
0.25	397.0	1075.6	2099.8	3514.0	0.25	300.9	757.6	1462.0	2434.6
0.50	397.8	1070.4	2078.2	3479.7	0.50	297.9	748.0	1438.7	2395.7
0.75	399.3	1067.6	2061.8	3454.9	0.75	295.3	740.4	1419.3	2366.0
1.00	401.2	1067.2*	2050.3	3439.2	1.00	293.2	734.6	1403.5	2342.4
1.25	403.8	1069.2	2044.0	3432.9*	1.25	291.6	730.9	1391.8	2326.1
1.50	406.9	1073.6	2042.6*	3435.7	1.50	290.4	729.0	1383.7*	2316.7
1.75	410.5	1080.5	2046.3	3448.0	1.75	289.7	729.0*	1379.5	2314.6*
2.00	414.7	1089.8	2055.1	3469.4	2.00	289.5*	731.0	1379.1	2319.6
3.00	436.9	1151.2	2140.4	3648.1	3.00	293.3	757.9	1415.7	2411.0
β	1.0	.99	0.96	0.97		0.95	0.95	0.93	0.93

	700mbs					850mbs			
α	12hr	24hr	36hr	48hr	α	12hr	24hr	36hr	48hr
0.0	247.4	608.1	1088.9	1592.6	0.0	244.3	601.9	1022.6	1417.5
0.25	243.3	596.6	1065.2	1559.5	0.25	239.7	588.6	997.6	1386.1
0.50	239.7	586.7	1044.1	1530.7	0.50	235.5	576.8	975.1	1358.5
0.75	236.4	578.4	1025.7	1505.4	0.75	231.6	566.5	955.1	1334.8
1.00	233.5	571.6	1009.8	1485.6	1.00	228.2	557.7	937.4	1315.0
1.25	231.0	566.3	996.6	1471.2	1.25	225.1	550.4	922.2	1299.0
1.50	228.9	562.7	986.0	1460.3	1.50	222.4	544.5	909.4	1285.9
1.75	227.2	560.6	978.0	1453.8	1.75	220.0	540.2	899.0	1278.7
2.00	225.8	560.0*	972.6*	1451.7*	2.00	218.1	537.3*	891.2	1274.3*
3.00	224.3*	573.3	977.1	1487.9	3.00	214.0*	540.7	884.1*	1295.8
β	0.91	0.92	0.89	0.91		0.88	0.89	0.86	0.90

These differences are small (especially if converted into an rms value) but show a significant pattern.

- Larger values of the force are suggested at low levels.
- The values of β suggest that at these short forecast ranges, it is the lower layers that will benefit most.

The drag on the atmosphere represents a "loss" of momentum by the atmosphere. The height at which this momentum is abstracted is conceivably of considerable importance. [The simple assumption (7) distributes the loss uniformly at all heights.] One of the theories for determining this level is based on the linear theory for steady state gravity waves in a flow in which the basic current $\bar{u}(z)$ varies with height (Eliassen and Palm, 1961; Bretherton, 1969). According to this theory, the otherwise uniform value of τ in the vertical is interrupted at the altitude where the ambient wind component in the direction of the low-level forcing wind changes sign. This is referred to as a zero wind line.

To investigate this in a retrospective manner, all of the 27 initial distributions of isobsric height were inspected, at all standard levels, to determine, in each grid-point column over North America, the altitude at which the geostrophic wind first had a component opposed to that of the geostrophic wind at 850 mbs. (For lack of a better name, this will be called wind reversal.) The 27 cases were then divided into 15 cases (FR) that had fewer than 75 grid points with the reversal level at or below 500 mbs, and 12 cases (MR) for which more than 75 such grid columns experienced a wind reversal below 500 mbs. (Figure 6 shows the field of the number of wind reversals by 500 mbs as it occurred in the full 27 case sample. Wind reversals over the ocean are presumably irrelevant.)

Table 2 shows the distribution of forecast error as a function of the number of wind reversals-- few (FR) or many (MR) . Values are shown for the shortest (12hr) and longest (48hr) forecast intervals.

Table 2. Squared height errors stratified by the number of wind reversals at or below 500 mbs over North America. (See text). β is the ratio of the squared height error to that for $\alpha = 0$.

	12-hour forecasts								48-hour forecasts							
	250		500		700m		850		250		500		700		850	
	FR	MR	FR	MR	FR	MR	FR	MR	FR	MR	FR	MR	FR	MR	FR	MR
$\alpha = 0$	434	350	322	282	255	238	242	246	3512	3617	2342	2656	1479	1742	1350	1510
$\alpha = 1.0$	440	353	314	267	242	223	228	228	3414	3474	2231	2486	1389	1617	1258	1395
β =	1.01	1.01	.98	.95	.95	.93	.94	.93	.97	.96	.95	.94	.94	.93	.93	.92
$\alpha = 3.0$	478	386	320	260	236	210	216	211	3651	3647	2347	2495	1426	1573	1268	1339
β =	1.10	1.10	.99	.92	.93	.88	.89	.86	1.04	1.01	1.00	.94	.96	.90	.94	.89

The β values show a small, but uniform tendency for

- the error reduction to be slightly greater when there are "more" wind reversals below 500 mbs, than when there are "few".

The general conclusion from this study is that there is indeed a benefit to be gained from introducing the effect of mountain wave drag into the Nested Grid Model. In particular, a revised test is indicated, in which greater consideration is given to theoretical ideas about the altitude at which the lost momentum is abstracted from the atmosphere. Mechanisms that effect the lower troposphere would seem to especially important.

REFERENCES

Bretherton,F.,1969: Momentum transport by gravity waves. Quart. J. R. Met. Soc., 95, 213-243,

Eliassen, A., and E. Palm, 1961: On the transfer of energy in stationary mountain waves. Geofys. Publ., 22, No. 3, 1-23.

Palmer, T., G. Shutts and R. Swinbank, 1986: Alleviation of a systematic westerly bias in general circulation and numerical weather prediction models through an orographic gravity wave drag parameterization. Quart. J. R. Met. Soc., 112, 1001,1039.

Pierrehumbert, R., 1987: Parameterization of Gravity Wave Drag (A working paper). Geophysical Fluid Dynamics Laboratory (unpublished).

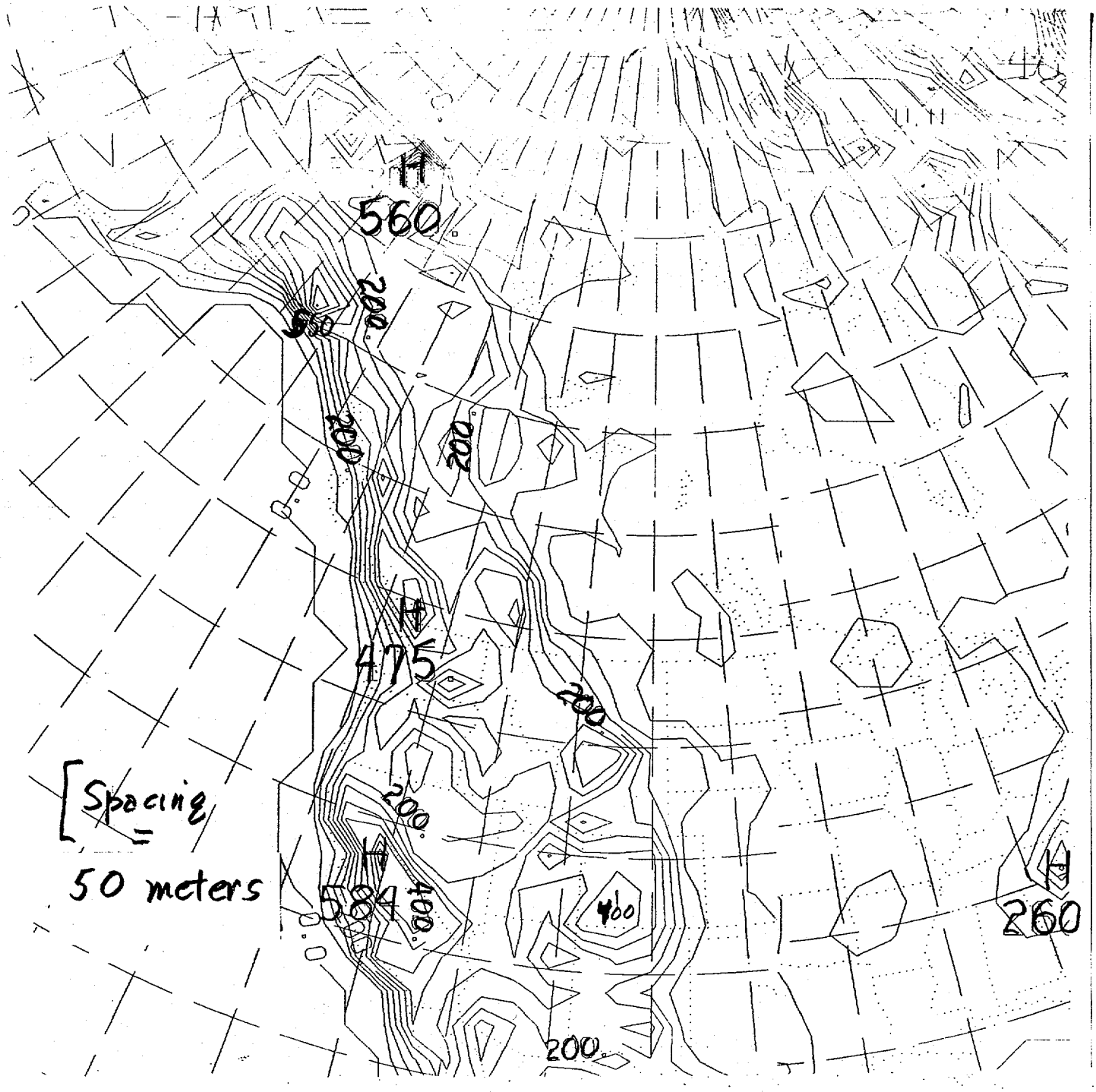

Figure 1. Standard deviation of ground height (meter) computed from the U. S. Navy tape of 10' by 10' orographic heights. The deviation was defined about the local averaged over a one-degree square.

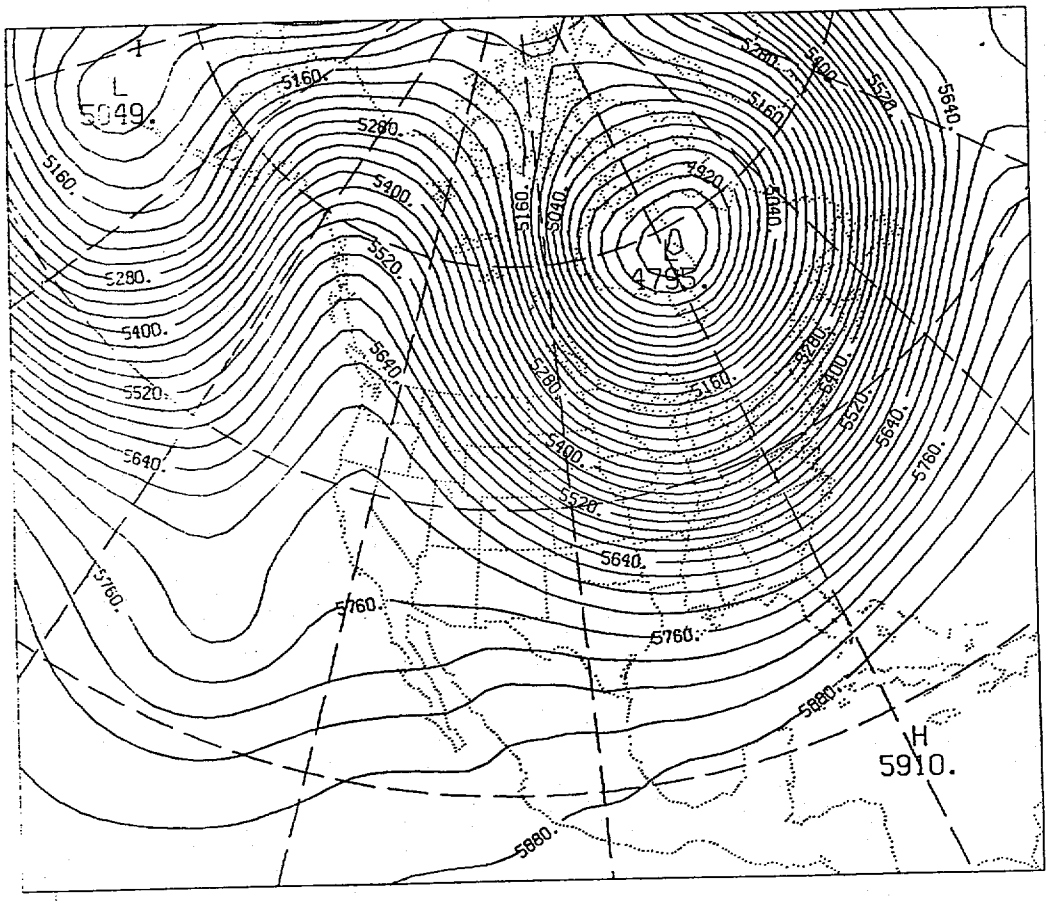

Figure 2. Mean height field at 500 mbs during the period

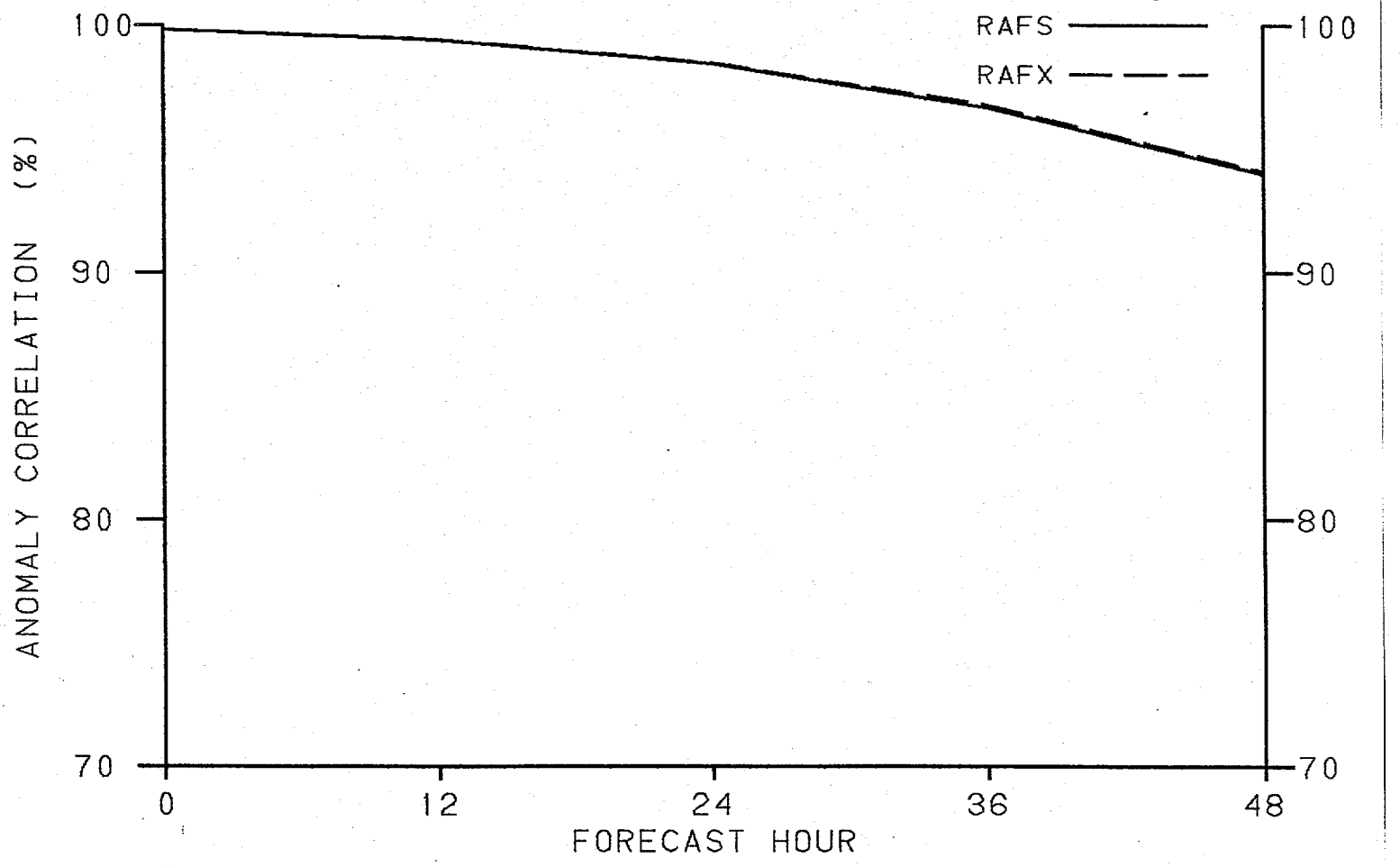

Figure 3. Variation of anomaly correlation coefficient with length of forecsst during the period

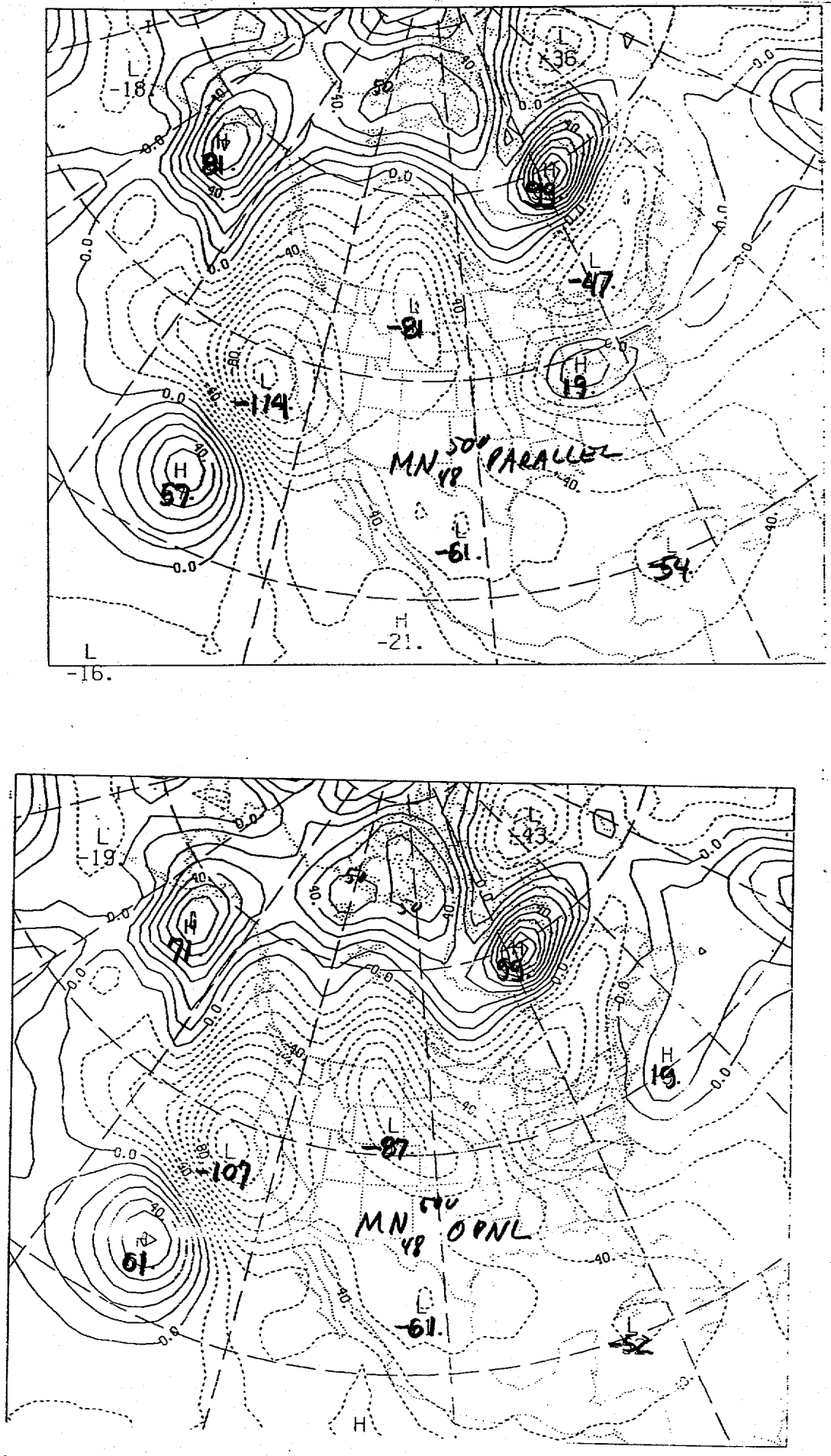

Figure 4. Mean 48-hour height errors at 500 mbs for the parallel (upper diagram) and operational (lower diagram) forecasts during the test period. Units = meters.

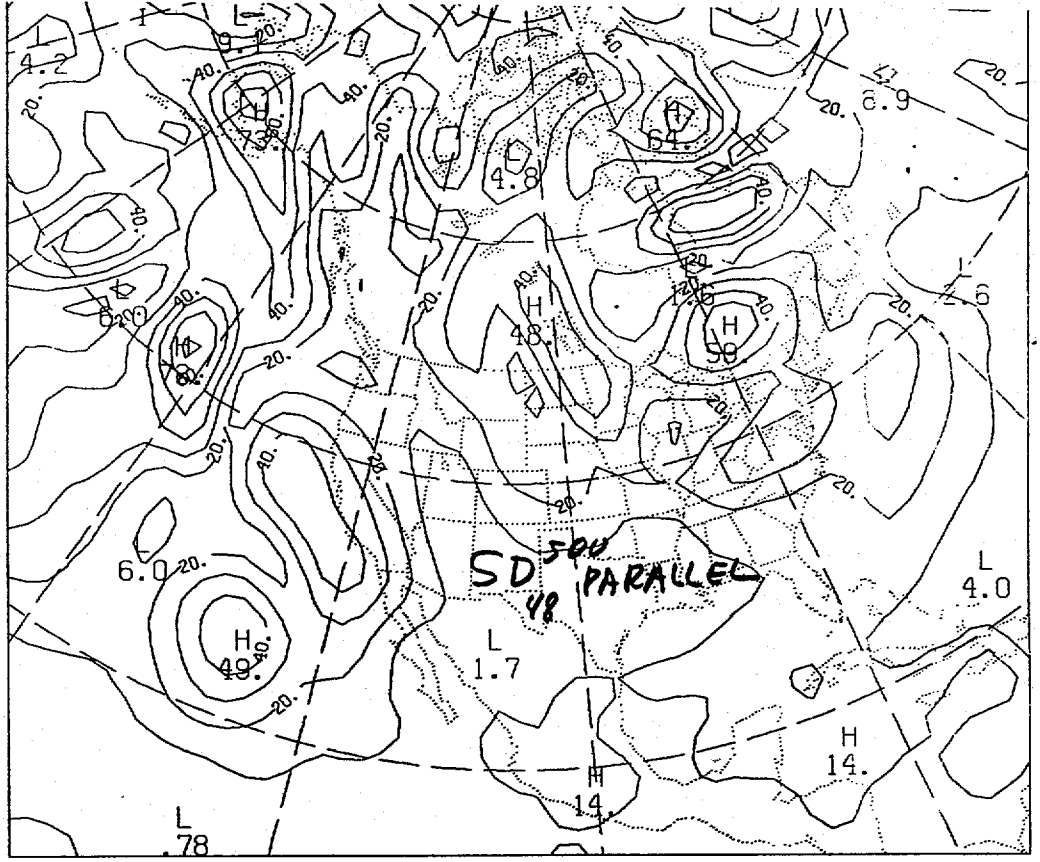

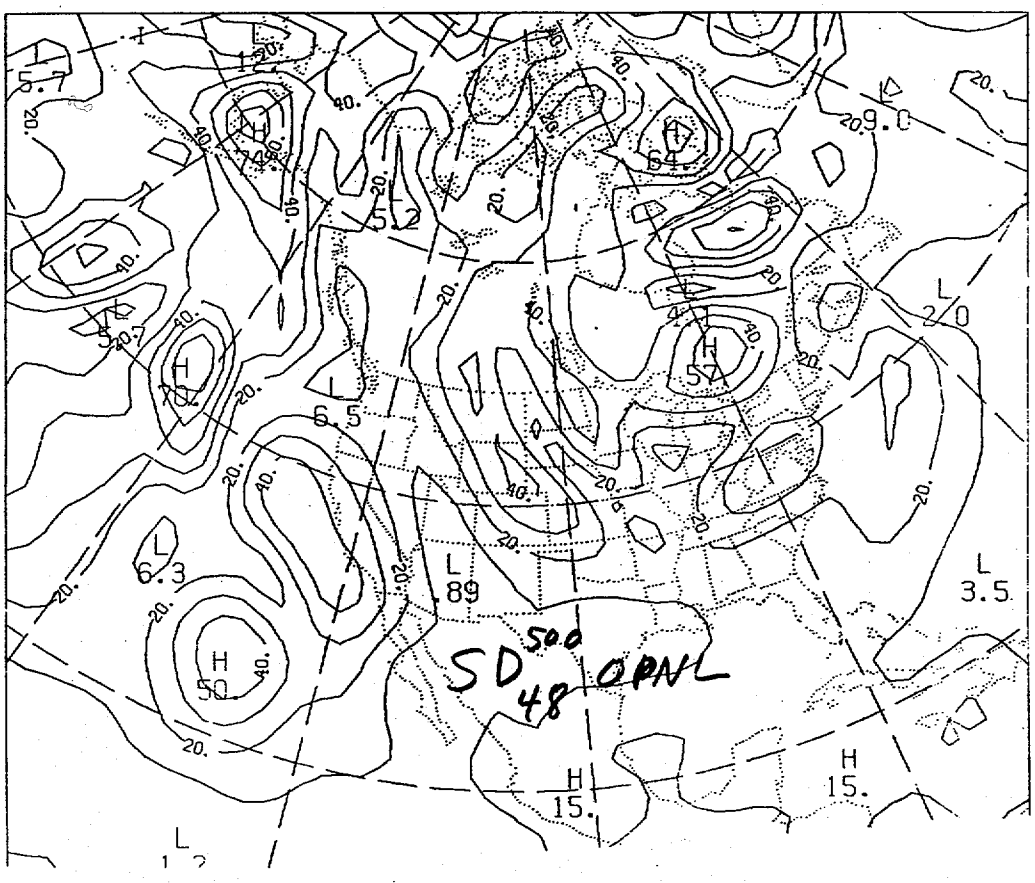

Figure 5. Standard deviation of 48-hour height errors at 500 mbs (meters) for the parallel (upper diagram) and operational (lower diagram) during the test period.

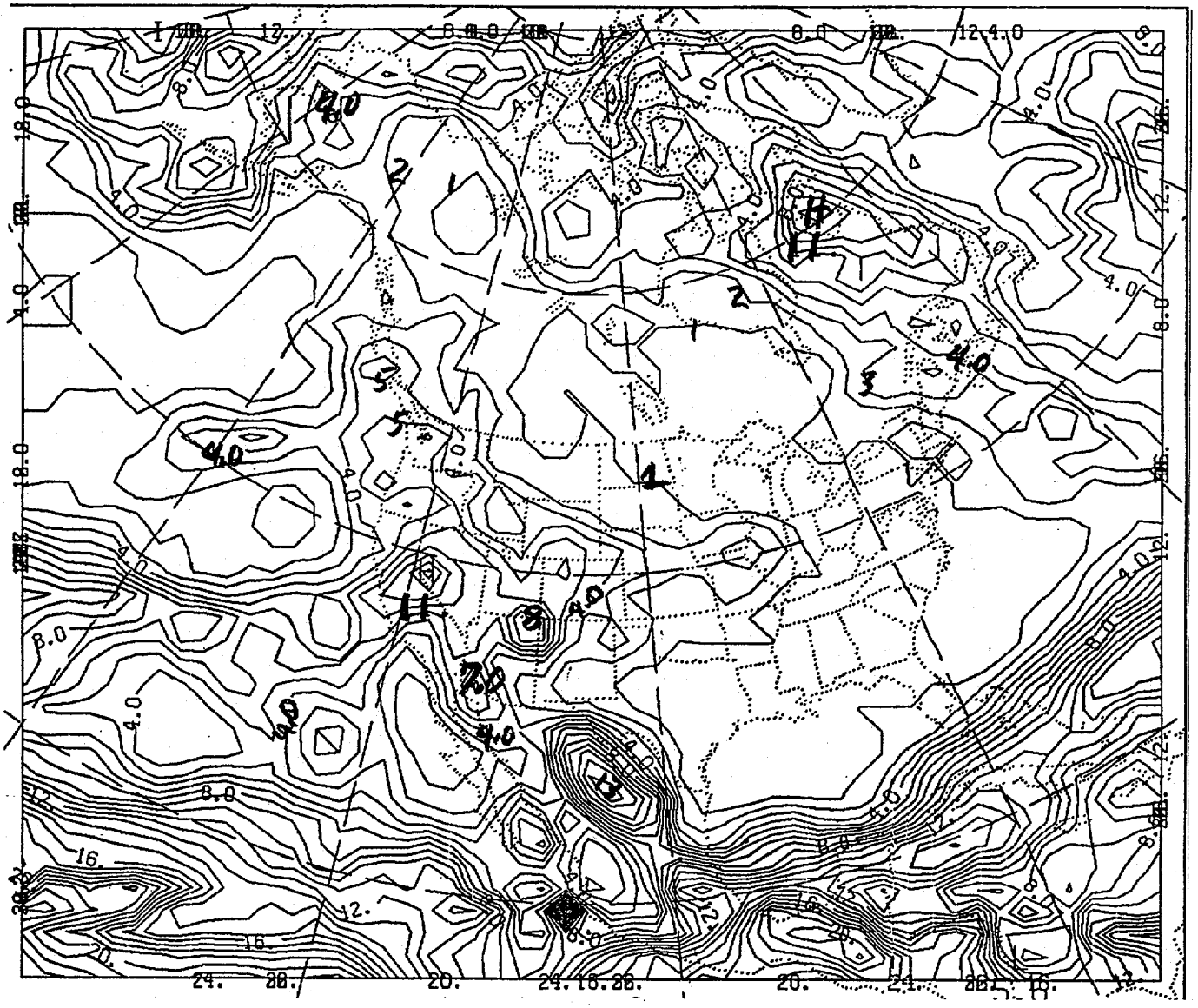

Figure 6. Distribution of geostrophic wind reversals at or below 500 mbs during the test period.